Solid-State Source of Nonclassical Photon Pairs with Embedded Multimode Quantum Memory

Kutlu Kutluer,[1] Margherita Mazzera,[1,*] and Hugues de Riedmatten[1,2]
[1]*ICFO-Institut de Ciencies Fotoniques, the Barcelona Institute of Science and Technology, Mediterranean Technology Park, 08860 Castelldefels (Barcelona), Spain*
[2]*ICREA-Institució Catalana de Recerca i Estudis Avançats, 08015 Barcelona, Spain*
(Received 2 February 2017; published 24 May 2017)

The generation and distribution of quantum correlations between photonic qubits is a key resource in quantum information science. For applications in quantum networks and quantum repeaters, it is required that these quantum correlations be stored in a quantum memory. In 2001, Duan, Lukin, Cirac, and Zoller (DLCZ) proposed a scheme combining a correlated photon-pair source and a quantum memory in atomic gases, which has enabled fast progress towards elementary quantum networks. In this Letter, we demonstrate a solid-state source of correlated photon pairs with embedded spin-wave quantum memory, using a rare-earth-ion-doped crystal. We show strong quantum correlations between the photons, high enough for performing quantum communication. Unlike the original DLCZ proposal, our scheme is inherently multimode thanks to a built-in rephasing mechanism, allowing us to demonstrate storage of 11 temporal modes. These results represent an important step towards the realization of complex quantum networks architectures using solid-state resources.

DOI: 10.1103/PhysRevLett.118.210502

Photonic quantum memories (QMs) play a central role in quantum information science, where they are used as quantum interfaces between flying and stationary qubits [1]. Rare-earth-ion-doped solids (REIDS) are interesting candidates as QMs as they feature long coherence times [2,3] and prospects for integration [4–7]. Most of the experiments to date in REIDS have demonstrated read-write quantum memories, where external quantum states of light are mapped on the QM [4,8–11]. This process requires the generation of a single photon or entangled photons by an external source with demanding spectral properties to achieve strong interactions between the quantum light and the QM [12]. An alternative solution has been proposed [13] which combines a photon-pair source and a quantum memory in a single physical system, an atomic gas. It is based on the creation of a single collective spin excitation (spin wave) via off-resonant spontaneous Raman scattering, heralded by the detection of a Stokes photon. After a programmable storage time, the spin wave can be transferred with high efficiency into a single anti-Stokes photon using a resonant read pulse. This scheme, in principle, leads to higher efficiencies than read-write QMs for the same optical depth, as the write-in stage is avoided [1]. Since the first demonstration [14], impressive progress has been realized, including the demonstration of elementary quantum networks [15–20], entanglement between four atomic ensembles [21], and long-lived quantum memories [22,23]. These demonstrations have made cold atomic ensembles one of the most advanced systems to date for quantum-network applications. The Duan, Lukin, Cirac, and Zoller (DLCZ) scheme has also been implemented with phonons in diamond [24] and in a mechanical resonator [25].

Schemes to combine QMs and photon-pair sources in rare-earth-ion-doped solid-state ensembles have also been proposed [26,27]. REIDS have much weaker optical transitions than atomic gases (their dipole moments are 2–3 orders of magnitude lower than alkali atoms), making off-resonant excitation challenging [28]. A solution is to excite atoms on resonance to achieve stronger interaction. However, this leads to fast dephasing due to inhomogeneous broadening of the optical transition in the crystal, making a rephasing mechanism mandatory to recover the collective emission of the second photon [26,27]. Early demonstrations of time-separated correlations between a crystal and a light field have been reported [29,30] using the scheme of Ref. [26], including entanglement between a light field and a solid-state spin-wave QM [31]. In these experiments, quantum correlations were demonstrated in the continuous-variable regime using heterodyne detection techniques.

Here, we demonstrate a temporally multimode DLCZ-like scheme [27] in the photon-counting regime in a rare-earth-ion-doped quantum memory. We generate pairs of correlated photons with a controllable delay and demonstrate quantum correlations between the photons for delays up to 20 μs. The photon pairs are created through spin-wave storage, effectively generating quantum correlations between single photons and single collective spin waves in the crystal. We also show experimentally that combining the DLCZ scheme with rephasing techniques allows for the creation of spin waves into multiple temporal modes. The use of photon-counting detection, which enables discrete variable encoding,

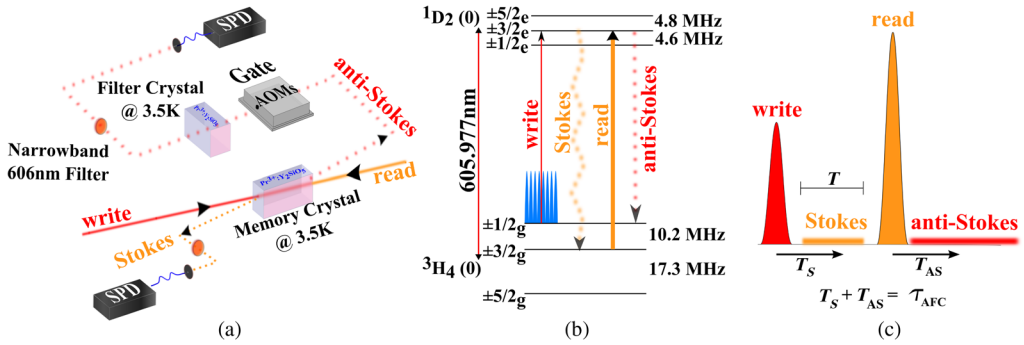

FIG. 1. (a) The experimental setup. The memory crystal, a 5-mm-long, 0.05%-doped Pr^{3+}:YSO, is hosted in a Montana Instruments Cryostation. The write and read pulses are counterpropagating. Their polarization is rotated along the D_2 crystal axis in order to maximize the absorption. Narrow-band filters at 600 nm (width 10 nm) are placed on both Stokes and anti-Stokes modes. The Stokes photons are fiber coupled to the detector with about 75% transmission. The anti-Stokes photons are first temporally gated by two acoustic optical modulators (AOMs) and later spectrally filtered by a 1-MHz-wide spectral hole at the $1/2_g$-$3/2_e$ transition frequency burned in a second Pr^{3+}:YSO crystal, 3 mm long, also at 3.5 K. The total transmission in the anti-Stokes arm, from the cryostat to the detector, is typically 24%. We use two silicon single-photon detectors (SPDs) for the detection of both photons. (b) Hyperfine splitting of the first sublevels (0) of the ground $^3H_4$ and the excited $^1D_2$ manifolds of Pr^{3+} in Y_2SiO_5. The AFC structure (blue comb) is prepared with the read mode. (c) Temporal pulse sequence. The write pulses are 1 μs long (FWHM), and have a negative frequency chirp with a hyperbolic tangent waveform of 800 kHz. The read pulses, sent 8 μs after the write pulses, have power of 24 mW, duration of 900 ns (FWHM), and frequency chirp of +800 kHz with a hyperbolic tangent waveform. T_S (T_{AS}) is the time separation between a Stokes (anti-Stokes) photon and the write (read) pulse. T is the width of the Stokes detection window. For one AFC preparation we send 500 write-read pairs every 313 μs for $P_w \leq 128$ μW. For higher P_w we decrease the number of trials to prevent deterioration of the AFC.

combined with the high quantum correlations demonstrated, makes our source of photon pairs with embedded quantum memory directly usable for quantum repeater schemes.

In our experiment, the rephasing mechanism uses the atomic frequency comb (AFC) scheme. It relies on the spectral tailoring of the inhomogeneous absorption profile as comblike structures with a spectral periodicity Δ, which rephase the ions at time $\tau_{\mathrm{AFC}} = 1/\Delta$ and lead to a collective emission [32,33]. The sample used is a Pr^{3+}: Y_2SiO_5 (Pr^{3+}:YSO) crystal cooled down to 3.5 K. Figure 1 shows the experimental setup [Fig. 1(a)] and the relevant energy level scheme of the crystal [Fig. 1(b)]. We first prepare an AFC on the $1/2_g$-$3/2_e$ transition, with $\tau_{\mathrm{AFC}} = 8$ μs. At the same time the $3/2_g$ state is emptied for the single-spin excitation (see [34]). Then we start a progression of trials, each consisting of the pulse sequence depicted in Fig. 1(c). We send write pulses resonant with the AFC and, after 1.4 μs, we open the gate to detect the Stokes photons. These are emitted in the whole solid angle, but we only collect the Stokes field backward at an angle of $\sim 4°$ with respect to the write mode. With our filtering system we mostly collect only photons resonant to the $^1D_2(0) \rightarrow {}^3H_4(0)$ transition. Then, we unconditionally send strong read pulses. The write and read pulses are counterpropagating; therefore, because of the phase-matching condition ($\vec{k}_{\mathrm{AS}} = \vec{k}_w + \vec{k}_r - \vec{k}_{\mathrm{S}}$) and collective interference, the anti-Stokes photons are emitted as counterpropagating with respect to the detected Stokes photon. The anti-Stokes photons are temporally and spectrally filtered before being steered to the detection stage.

We start our measurements by characterizing the light emitted in the Stokes mode. Figure 2(a) shows the temporal Stokes histogram in a 2-μs window, for a write power $P_w = 16$ μW. Figure 2(b) shows the spectrum of the emitted Stokes field, from which we infer that the hyperfine branching ratio of the Stokes photons, β_{BR}, at the relevant $3/2_g$-$3/2_e$ transition frequency is about 60% (see [34]). We also measure the probability to generate a Stokes photon P_{S} as a function of P_w, as shown in Fig. 2(c). We observe a linear dependence, as predicted in [27] for $P_{\mathrm{S}} \ll 1$. These observations suggest that the light emitted in the Stokes mode comes from the direct excitation of the ions by the write pulse. Figure 2(d) also shows the time histogram of the anti-Stokes mode after sending the read pulse.

We now look for coincidence detection between the Stokes and anti-Stokes modes. The Stokes photon, which heralds a single-spin excitation, is emitted from the ions that have spent a time T_{S} in the excited state. After a storage time t_s in the spin state, the read pulse then transfers the collective excitation from the spin state back to the excited state. At that moment, the phase evolution in the excited state resumes, and the correlated anti-Stokes photon will be emitted at time T_{AS} after the read pulse, such that $T_{\mathrm{S}} + T_{\mathrm{AS}} = \tau_{\mathrm{AFC}}$. We record the detection times of the Stokes (T_{S}) and anti-Stokes (T_{AS}) photons, and plot a histogram of the coincidences as a function of the sum $T_{\mathrm{S}} + T_{\mathrm{AS}}$. For correlated pairs, we therefore expect a coincidence peak at $T_{\mathrm{S}} + T_{\mathrm{AS}} = \tau_{\mathrm{AFC}}$. Figure 3(a) shows such a histogram for $P_w = 16$ μW, where we see a clear correlation peak around $\tau_{\mathrm{AFC}} = 8$ μs.

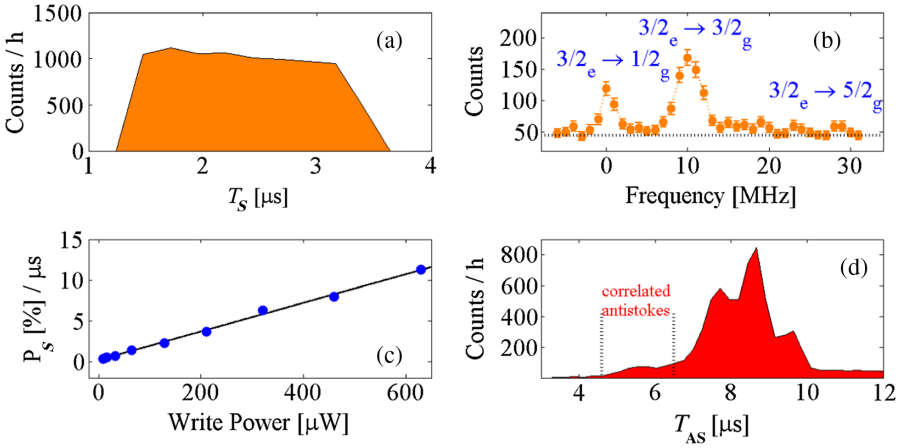

FIG. 2. (a) Stokes count rate in a 2-μs detection window, for $P_w = 16$ μW. (b) Stokes counts as a function of the position of a 1-MHz-wide spectral hole burned in the filter crystal. The 0 frequency corresponds to the frequency of the write pulse. The dotted gray horizontal line is the noise given by the detector dark counts. (c) Probability to create Stokes photons as a function of the write pulse power. The solid curve is a linear fit of the experimental data points. (d) Anti-Stokes count rate. The dotted vertical bars indicate the temporal mode where the anti-Stokes photons correlated to the Stokes photons of panel (a) should lie to satisfy the condition $T_S + T_{AS} = \tau_{AFC}$. This histogram shows a peak at around 8.5 μs originated from the second echo of the write pulse leaked into the anti-Stokes mode. Note that this peak is not in the temporal mode of the correlated anti-Stokes photons. Nevertheless, from the Gaussian fit of the two peaks we infer a contribution to the anti-Stokes counts of around 4%.

To quantify the correlation between Stokes and anti-Stokes photons, we measure intensity correlation functions. The second-order cross-correlation function $g^{(2)}_{S,AS}$ is defined as $g^{(2)}_{S,AS} = p_{S,AS}/(p_S p_{AS})$, where $p_{S,AS}$ is the probability to detect a coincidence between Stokes and anti-Stokes photons and p_S (p_{AS}) is the probability to detect a Stokes (anti-Stokes) photon. To infer $g^{(2)}_{S,AS}$, we measure the number of coincidences in a time window $\Delta\tau$ around $T_S + T_{AS} = \tau_{AFC}$ in the same trial, and we compare this number with the accidental coincidences recorded for Stokes and anti-Stokes photon emitted in different independent trials. An example is shown in Fig. 3(b) for

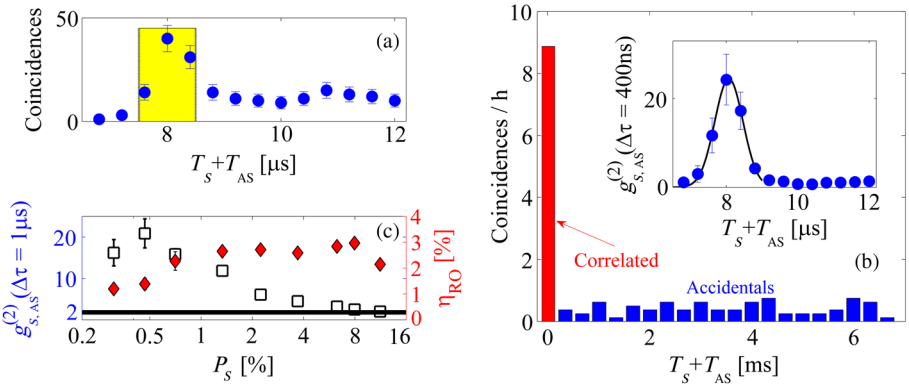

FIG. 3. (a) Coincidence counts between Stokes and anti-Stokes photons as a function of the sum $T_S + T_{AS}$. The bin size is $\Delta\tau = 400$ ns. The shaded area indicates the time window used to calculate the $g^{(2)}_{S,AS}(\Delta\tau = 1\ \mu s)$ value. We also observe a smaller peak at 11 μs, due to the noise generated by the second AFC echo of the write pulse [see Fig. 2(d)]. However, this peak is also present when Stokes and anti-Stokes photons are detected in different trials and, therefore, does not correspond to correlated photons. (b) Coincidence counts per hour between Stokes and anti-Stokes photons in the 1-μs-wide temporal mode around $T_S + T_{AS} = \tau_{AFC} = 8$ μs in the same storage trial (bar at 0) and in different storage trials separated by multiples of 313 μs. The $g^{(2)}_{S,AS}$ value is calculated as the ratio between the coincidences in the same storage trial and the average of the coincidences in different storage trials. The inset shows the peak in the $g^{(2)}_{S,AS}$ with a bin size of $\Delta\tau = 400$ ns. The fit of the correlation peak to a Gaussian curve, done over a 2-μs window around the peak, is also shown. (c) $g^{(2)}_{S,AS}$ value (squares) and readout efficiency (diamonds) as a function of the Stokes creation probability, P_S, calculated by the raw detection counts backpropagated at the crystal using known losses. The black horizontal line sets the classical threshold for the $g^{(2)}_{S,AS}$ given by the Cauchy-Schwarz inequality.

$P_w = 16\ \mu W$ and $\Delta\tau = 1\ \mu$s, which includes approximately 76% of the total peak counts. For this particular example, with average $t_s = 5.6\,\mu$s, we find $g^{(2)}_{S,AS}(\Delta\tau = 1\,\mu s) = 21 \pm 4$. This is much higher than the threshold of approximately 6 that enables the violation of a Bell inequality if at least two modes are stored [37]. The inset in Fig. 3(b) shows a zoom on the correlation peak for a smaller $\Delta\tau = 400$ ns, leading to $g^{(2)}_{S,AS}(\Delta\tau = 400\ \text{ns}) = 24 \pm 6$. The shape of the normalized correlation peak is fitted with a Gaussian curve and a temporal FWHM of (940 ± 100) ns is extracted. This is close to the expected width corresponding to the write-pulse duration convoluted with the time-bin size.

To further characterize our system, we measure $g^{(2)}_{S,AS}(\Delta t = 1\ \mu s)$ as a function of P_S [Fig. 3(c)], which can be adjusted by tuning P_w [see Fig. 2(c)]. We observe a reduction of the $g^{(2)}_{S,AS}$ value when P_S is increased, as expected for a DLCZ-like process. At lower P_S, the rate of Stokes photons becomes comparable to the noise and the value of $g^{(2)}_{S,AS}$ decreases. We also measure the readout efficiency $\eta_{RO} = (p_{S,AS} - p^{acc}_{S,AS})/p_S$ as a function of P_S, where $p^{acc}_{S,AS}$ is the accidental coincidence probability. We observe a linear increase up to $P_S = 1\%$, due to the noise in the Stokes mode. Afterwards it stays constant around 3%, close to the expected value (see [34]). This value is comparable to the readout efficiency achieved in the latest demonstration of continuous-variable entanglement between light and spin waves implemented in the same system [31].

To prove unambiguously the nonclassical correlations between the two photons, we use the Cauchy-Schwarz inequality

$$R = \frac{(g^{(2)}_{S,AS})^2}{g^{(2)}_{S,S} g^{(2)}_{AS,AS}} \leq 1,$$

where $g^{(2)}_{S,S}$ and $g^{(2)}_{AS,AS}$ are second-order autocorrelation functions of Stokes and anti-Stokes photons, respectively. To measure these quantities, we introduce a 50:50 fiber splitter and two SPDs in the Stokes (anti-Stokes) arm and proceed in a similar way as for the cross-correlation. With $P_w = 64\ \mu$W, we find $g^{(2)}_{S,S}(\Delta t = 1\,\mu s) = 1.85 \pm 0.36$, $g^{(2)}_{AS,AS}(\Delta t = 1\,\mu s) = 1.75 \pm 0.57$, and $g^{(2)}_{S,AS}(\Delta t = 1\ \mu s) = 11.9 \pm 0.9$. Eventually we find $R = 44 \pm 20$, which exceeds the classical limit by more than 2 standard deviations.

To show that the delay between the Stokes and anti-Stokes photons can be controlled, we measure the retrieval efficiency as a function of the storage time in the spin state t_s, as shown in Fig. 4(a). The data are fitted with a Gaussian curve, from which we extract a $1/e$ decay constant of $(8.3 \pm 0.8)\ \mu$s. This decay is likely due to inhomogeneous broadening of the spin transition. The same measurement in a standard spin-wave AFC experiment in this crystal gives a similar value of $(9.9 \pm 1.5)\ \mu$s. The decay in η_{RO} also affects $g^{(2)}_{S,AS}$, as shown in Fig. 4(b). Nevertheless, we observe nonclassical correlation for t_s up to 12 μs, corresponding to a total storage time of $t_s + \tau_{AFC} = 20\ \mu$s.

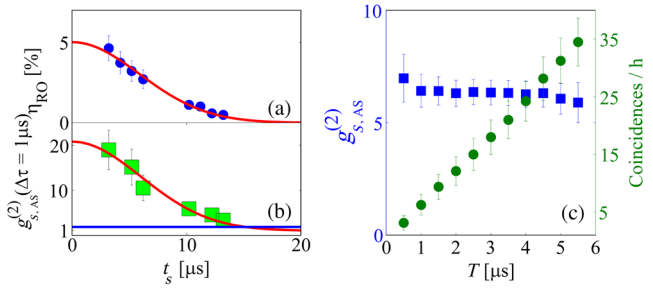

FIG. 4. Readout efficiency (a) and $g^{(2)}_{S,AS}(\Delta t = 1\ \mu s)$ cross-correlation values (b) as a function of the storage time in the spin state t_s. The red line is the fit of the experimental data to a Gaussian decay, which gives a $1/e$ decay time of $(8.3 \pm 0.8)\ \mu$s, corresponding to a spin-inhomogeneous linewidth of 45 ± 2 kHz (44 ± 4 kHz for $g^{(2)}_{S,AS}$). For this curve, we do not subtract the accidental counts. The blue horizontal line in (b) sets the classical threshold for the $g^{(2)}_{S,AS}$ given by the Cauchy-Schwarz inequality. (c) $g^{(2)}_{S,AS}(\Delta t = 1\ \mu s)$ cross-correlation (squares) and coincidence counts per hour (circles) between the Stokes and anti-Stokes photons as a function of Stokes window size, T. The total Stokes window size is 5.5 μs. In the data processing stage we adjust the Stokes window size as multiples of the duration of the write pulse (FWHM = 500 ns). The values are averages of all possible windows for different window sizes, e.g., 11 for a 500-ns window, 9 for a 150-ns window, etc. In this measurement $P_w = 64\ \mu$W. The read pulse is sent 15 μs after the write pulse. The decrease on $g^{(2)}_{S,AS}$ with respect to the one in Fig. 3(a) is due to the longer spin-state storage time and less-efficient readout for a shorter write pulse ($\eta_{RO} = 1\%$).

Finally, we discuss the temporal multimode nature of our source. The detection of a Stokes photon at a different time $T_S{}'$ creates a spin wave that will also rephase at a different time T'_{AS}, still preserving $T_S{}' + T'_{AS} = \tau_{AFC}$. The maximal number of modes is given by $N_m = T/\Delta\tau$, where T is the detection window of the Stokes photons. Note that there is a trade-off between the number of modes and the readout efficiency of each mode. The efficiency is maximized if $\Delta\tau$ is bigger than the correlation peak. In our case, we choose $\Delta\tau$ comparable to the FWHM of the peak. Figure 4(c) shows the coincidence count rate and the $g^{(2)}_{S,AS}$ as a function of T. We observe a linear increase in coincidence count rate while increasing T. At the same time, the $g^{(2)}_{S,AS}$ values stay constant. This shows an important feature of our scheme: adding more temporal modes increases the coincidence rate but does not decrease the correlation. The maximal number of modes in our current experiment is $N_m = T/\Delta\tau = 11$ modes, a factor of 5 improvement with respect to previous multimode DLCZ-like experiments [31,38].

Several improvements to our system are possible. The Stokes probability could be improved, without resorting to

higher write-pulse powers. For example, longer crystals or, to some extent, higher concentrations could be employed to achieve higher optical depth. The light-atom interaction could also be enhanced with external cavities. These measures would also be beneficial for the readout efficiency. This latter could be further boosted by filtering the Stokes photon for suppression of wrong heralds, by improving the quality of the AFC for better rephasing, and by optimizing the transfer efficiency. The storage time could be greatly improved using spin-echo techniques [39], with prospects of up to tens of seconds in our crystal [2] or hours in europium-ion-doped crystals [3]. Even though the emitted photons are at 606 nm, it is possible to efficiently convert them to telecom *C*-band wavelengths using quantum frequency-conversion techniques [40].

Our observation of nonclassical correlations between photon pairs emitted from a solid-state ensemble with a controllable delay by using photon-counting techniques represents an important achievement towards scalable quantum repeater architectures. The demonstrated inherent temporal multimodality of our protocol also paves the way towards the heralded entanglement of remote solids with temporal multiplexing, which can greatly enhance the distribution rate of entanglement [41].

We acknowledge financial support by the ERC starting grant QuLIMA, by the Spanish Ministry of Economy and Competitiveness (MINECO) and Fondo Europeo de Desarrollo Regional (FEDER) (Grant No. FIS2015-69535-R), by MINECO Severo Ochoa through Grant No. SEV-2015-0522, by AGAUR via Grant No. 2014 SGR 1554, by Fundació Cellex, and by CERCA Programme/Generalitat de Catalunya.

Note added in the proof—.We note that a similar work demonstrating the AFC-DLCZ protocol in an europium doped crystal has been performed independently and is published alongside the present Letter [42].

*margherita.mazzera@icfo.es

[1] M. Afzelius, N. Gisin, and H. de Riedmatten, Phys. Today **68**, No. 12, 42 (2015).
[2] G. Heinze, C. Hubrich, and T. Halfmann, Phys. Rev. Lett. **111**, 033601 (2013).
[3] M. Zhong, M. P. Hedges, R. L. Ahlefeldt, J. G. Bartholomew, S. E. Beavan, S. M. Wittig, J. J. Longdell, and M. J. Sellars, Nature (London) **517**, 177 (2015).
[4] E. Saglamyurek, N. Sinclair, J. Jin, J. A. Slater, D. Oblak, F. Bussières, M. George, R. Ricken, W. Sohler, and W. Tittel, Nature (London) **469**, 512 (2011).
[5] T. Zhong, J. M. Kindem, E. Miyazono, and A. Faraon, Nat. Commun. **6**, 8206 (2015).
[6] S. Marzban, J. G. Bartholomew, S. Madden, K. Vu, and M. J. Sellars, Phys. Rev. Lett. **115**, 013601 (2015).
[7] G. Corrielli, A. Seri, M. Mazzera, R. Osellame, and H. de Riedmatten, Phys. Rev. Applied **5**, 054013 (2016).
[8] C. Clausen, I. Usmani, F. Bussières, N. Sangouard, M. Afzelius, H. de Riedmatten, and N. Gisin, Nature (London) **469**, 508 (2011).
[9] D. Rieländer, K. Kutluer, P. M. Ledingham, M. Gündoğan, J. Fekete, M. Mazzera, and H. de Riedmatten, Phys. Rev. Lett. **112**, 040504 (2014).
[10] Z.-Q. Zhou, S. F. Huelga, C.-F. Li, and G.-C. Guo, Phys. Rev. Lett. **115**, 113002 (2015).
[11] A. Seri *et al.*, arXiv:1701.09004 [Phys. Rev. X (to be published)].
[12] D. Rieländer, A. Lenhard, M. Mazzera, and H. de Riedmatten, New J. Phys. **18**, 123013 (2016).
[13] L.-M. Duan, M. D. Lukin, J. I. Cirac, and P. Zoller, Nature (London) **414**, 413 (2001).
[14] A. Kuzmich, W. P. Bowen, A. D. Boozer, A. Boca, C. W. Chou, L.-M. Duan, and H. J. Kimble, Nature (London) **423**, 731 (2003).
[15] T. Chanelière, D. N. Matsukevich, S. D. Jenkins, S.-Y. Lan, T. A. B. Kennedy, and A. Kuzmich, Nature (London) **438**, 833 (2005).
[16] M. D. Eisaman, A. André, F. Massou, M. Fleischhauer, A. S. Zibrov, and M. D. Lukin, Nature (London) **438**, 837 (2005).
[17] C. W. Chou, H. de Riedmatten, D. Felinto, S. V. Polyakov, S. J. van Enk, and H. J. Kimble, Nature (London) **438**, 828 (2005).
[18] C.-W. Chou, J. Laurat, H. Deng, K. S. Choi, H. de Riedmatten, D. Felinto, and H. J. Kimble, Science **316**, 1316 (2007).
[19] K. S. Choi, H. Deng, J. Laurat, and H. J. Kimble, Nature (London) **452**, 67 (2008).
[20] Z.-S. Yuan, Y.-A. Chen, B. Zhao, S. Chen, J. Schmiedmayer, and J.-W. Pan, Nature (London) **454**, 1098 (2008).
[21] K. S. Choi, A. Goban, S. B. Papp, S. J. van Enk, and H. J. Kimble, Nature (London) **468**, 412 (2010).
[22] A. G. Radnaev, Y. O. Dudin, R. Zhao, H. H. Jen, S. D. Jenkins, A. Kuzmich, and T. A. B. Kennedy, Nat. Phys. **6**, 894 (2010).
[23] S.-J. Yang, X.-J. Wang, X.-H. Bao, and J.-W. Pan, Nat. Photon. **10**, 381 (2016).
[24] K. C. Lee, B. J. Sussman, M. R. Sprague, P. Michelberger, K. F. Reim, J. Nunn, N. K. Langford, P. J. Bustard, D. Jaksch, and I. A. Walmsley, Nat. Photon. **6**, 41 (2012).
[25] R. Riedinger, S. Hong, R. A. Norte, J. A. Slater, J. Shang, A. G. Krause, V. Anant, M. Aspelmeyer, and S. Gröblacher, Nature (London) **530**, 313 (2016).
[26] P. M. Ledingham, W. R. Naylor, J. J. Longdell, S. E. Beavan, and M. J. Sellars, Phys. Rev. A **81**, 012301 (2010).
[27] P. Sekatski, N. Sangouard, N. Gisin, H. de Riedmatten, and M. Afzelius, Phys. Rev. A **83**, 053840 (2011).
[28] E. A. Goldschmidt, S. E. Beavan, S. V. Polyakov, A. L. Migdall, and M. J. Sellars, Opt. Express **21**, 10087 (2013).
[29] P. M. Ledingham, W. R. Naylor, and J. J. Longdell, Phys. Rev. Lett. **109**, 093602 (2012).
[30] S. E. Beavan, M. P. Hedges, and M. J. Sellars, Phys. Rev. Lett. **109**, 093603 (2012).
[31] K. R. Ferguson, S. E. Beavan, J. J. Longdell, and M. J. Sellars, Phys. Rev. Lett. **117**, 020501 (2016).
[32] M. Afzelius, C. Simon, H. de Riedmatten, and N. Gisin, Phys. Rev. A **79**, 052329 (2009).

[33] H. de Riedmatten, M. Afzelius, M. U. Staudt, C. Simon, and N. Gisin, Nature (London) **456**, 773 (2008).
[34] See Supplemental Material at http://link.aps.org/supplemental/10.1103/PhysRevLett.118.210502, which includes Refs. [35,36], for details about the preparation of the atomic frequency comb and the calculation of the readout efficiency.
[35] M. Bonarota, J. Ruggiero, J.-L. Le Gouët, and T. Chanelière, Phys. Rev. A **81**, 033803 (2010).
[36] P. Jobez, N. Timoney, C. Laplane, J. Etesse, A. Ferrier, P. Goldner, N. Gisin, and M. Afzelius, Phys. Rev. A **93**, 032327 (2016).
[37] H. de Riedmatten, J. Laurat, C. W. Chou, E. W. Schomburg, D. Felinto, and H. J. Kimble, Phys. Rev. Lett. **97**, 113603 (2006).
[38] B. Albrecht, P. Farrera, G. Heinze, M. Cristiani, and H. de Riedmatten, Phys. Rev. Lett. **115**, 160501 (2015).
[39] P. Jobez, C. Laplane, N. Timoney, N. Gisin, A. Ferrier, P. Goldner, and M. Afzelius, Phys. Rev. Lett. **114**, 230502 (2015).
[40] N. Maring, K. Kutluer, J. Cohen, M. Cristiani, M. Mazzera, P. M. Ledingham, and H. de Riedmatten, New J. Phys. **16**, 113021 (2014).
[41] C. Simon, H. de Riedmatten, M. Afzelius, N. Sangouard, H. Zbinden, and N. Gisin, Phys. Rev. Lett. **98**, 190503 (2007).
[42] C. Laplane, P. Jobez, J. Etesse, N. Gisin, and M. Afzelius, preceding Letter, Phys. Rev. Lett. **118**, 210501 (2017).